Journal of the Ceramic Society of Japan 116 [10] 1134-1138 2008 **Technical report**

Fabrication of ultra-compact Er-doped waveguide amplifier based on bismuthate glass

Motoshi ONO,† Yuki KONDO, Junichi KAGEYAMA and Naoki SUGIMOTO

Asahi Glass Co., Ltd. Research Center, 1150, Hazawa-cho, Kanagawa-ku, Yokohama-shi, Kanagawa 221–8755

Due to the possibility of high Er^{3+} doping and their broadband emission, the bithmuth-oxide-based glasses can be a promising candidate of host materials for a compact waveguide amplifier with high performance. By a novel fabrication process, we have developed a Bi_2O_3-based waveguide device with propagation loss as low as 0.13 dB/cm, which is comparable to the silica-based waveguides. We have achieved an ultra-compact Er-doped waveguide amplifier with 1 cm^2 size by designing a spiral light-wave circuit with low bending loss. This EDWA showed gain values over 15 dB, noise figures lower than 8 dB and gain flatness less than 2 dB over the whole C-band region. The output power of this EDWA reached higher than 12 dBm.

Key-words : Waveguide amplifier, Bismuth, Er, Waveguide, EDW

[Received June 9, 2008; Accepted September 11, 2008]

1. Introduction

As demand for higher bandwidth increases, the optical fiber communication systems are evolving from current point-to-point static links to dynamically reconfigured networks, such as optical burst switching (OBS) and optical packet switching (OPS) networks.[1),2)] As the signal power and wavelengths change along the traffic load, optical amplifiers used in such networks need to adapt to the changing signal levels in order to ensure error-free operation.

Another aspect of future optical nodes is that they will require many gain blocks to compensate for the losses in the optical switches. The number of gain blocks will increase as the node scales to larger switch port counts in order to achieve capacity of Tbps-order information. Up to now, Er-doped fiber amplifiers (EDFA) with different schemes have been demonstrated to control optical transients due to sudden change in number of channels.[3),4)] However, due to the required length and minimum bending radii of fibers for the gain-medium, it is generally difficult to pack many EDFAs within a compact space. Therefore, advances have been made on the fabrication techniques of Er-doped waveguide amplifiers (EDWA), and their potential applications in arrayed amplifiers and photonic integrated circuits are being considered.[5)–10)]

Bismathate glass has the ability of highly doping Er-ions, wide-band emission spectrum, easy refractive index control and high reliability. These excellent features are suitable for an amplifier devise with compact size and high performance. We have developed a fabrication process of low loss waveguide and achieved 0.13 dB/cm, which is as low as the silica-based waveguides. Furthermore, we have designed light wave circuits to downsize the waveguide amplifier. We designed and proposed two types of waveguide circuits within 1 cm^2 chip size circular spiral layout and square spiral one. After carefully examining the insertion loss and gain characteristics of these two layouts, it was confirmed that the circular spiral layout has better performance than the square spiral one. Because the square spiral layout has many inflection points, where large mode miss-match loss occurs. Then to optimize waveguide length, we have prepared three waveguides which length are 16 cm, 25 cm, and 32 cm, respectively. Finally, we have made a choice of the 25 cm long circular spiral layout for 1 cm^2 size Bi-EDW.

2. Experimental procedure

2.1 Fabricated of Bi-EDWA

Er-doped bismuth oxide glass films were prepared by RF magnetron sputtering in Ar/O_2 atmosphere. The host glass contains Bi_2O_3, SiO_2 and Ga_2O_3. Concentration of Er ions was 6250 ppm in weight. Substrates used here were soda lime silicate glass whose expansion coefficient is nearly the same as those of the core and clad films. We measured an emission spectrum of Bi_2O_3-based Er-doped glass film by pumping at 980 nm. To fabricate channel waveguides, reactive ion beam etching was used. To make a patterned photo-resist mask for dry etching, an ultraviolet laser (He-Cd laser) writing system was used. After dry etching, the photo-resist mask was removed by oxygen plasma ashing. The channel waveguides were covered with cladding film of 10 μm thickness by magnetron sputtering. Numerical aperture and Δ at 1304 nm of fabricated channel waveguide were 0.32 and 1.5%. The core width, height, and its refractive index were 5 μm, 3.3 μm, and 1.94, respectively. Propagation loss of the channel waveguide was measured by using the cut-back method at 1310 nm. In order to measure the gain characteristics of this straight Bi-EDWA, two laser diodes at 1480 nm were used to excite Er^{3+} ions in the Bi-EDW by bidirectional pumping. A tunable laser diode from 1520 to 1600 nm was used as a signal light source. Signal light through an isolator was coupled with the pump light by a 1480/1550 WDM coupler. The input and output port of the Bi-EDW were spliced with single channel fiber arrays by UV curing resin. High NA single mode fibers (HI980, Corning) were used for the fiber arrays and WDM couplers. The output signal from the Bi-EDW was introduced into an optical spectrum analyzer via an FC-coupled isolator. Device under test (DUT) was Bi-EDW including input and output fiber arrays.

† Corresponding author: M. Ono; E-mail: motoshi-ono@agc.co.jp

2.2 Downsizing of Bi-EDWA

We have investigated to get high gain value and downsize the Bi-EDWA. To get high gain value, the easiest way is to lengthen the waveguide circuits. But it leads enlarge the chip size. In order to obtain a high performance compact waveguide chip, we adopted a spiral layout. So we simulated and designed the low loss spiral layout waveguides to strike a balance between elongating and enlarging. First of all, we simulated the relationship between single-mode condition and Δ when single-mode beam was input to the waveguide.

Additionally, in order to determine the minimum curvature radius, we simulated the bending loss for each radius at maximum Δ satisfied single-mode condition. We proposed two types of waveguide circuits within 1 cm^2 chip size, circular spiral layout and square spiral one. Because square spiral layout has many inflection points, mode-mismatch loss are aboundingly generated. To reduce the mode-mismatch loss, an offset structure for the re-alignment of the mode center was introduced. Offset values minimalizing the mode-mismatch loss were simulated. All of the simulations were executed using the Beam Propagation Method (BPM).

Finally we fabricated two optimally designed spiral waveguide and evaluated them. For three waveguide lengths were measured of both layouts. The gain values were measured by the experimental setups described above.

3. Results and discussion

3.1 Emission spectrum of Bi_2O_3-based Er-doped glass film

Emission spectrum of Bi_2O_3-based Er-doped glass film pumped at 980 nm is shown in **Fig. 1**. Figure 1 also shows emission spectra of Er^{3+} ions in a SiO_2 glass and a phosphate glass. To compare the fluorescence bandwidth of the $4I_{13/2}$–$4I_{15/2}$ transition of Er^{3+} ions in each host glass, the fluorescence intensity is normalized by dividing with the peak intensity for each spectrum. The bandwidth of Bi_2O_3-based glass film was clearly broader than those of SiO_2 glass and phosphate glass. This result indicates that the Bi-EDW has a high potential as a broadband optical amplifier.

3.2 Characteristics of channel waveguides

In order to fabricate the bismuthate glass was dry-etched by fluorine containing gas and the atomic components of the bismuthate glass were fluorinated. Since many of these reaction products, namely fluorides, are nonvolatile, dry-etching of bismuthate glass is usually very difficult. In this section, we reported the loss characteristics of the channelwaveguides. **Figure 2** shows the waveguide-length dependence of the insertion loss the Bi-EDW, measured by cut-back method at 1310 nm. The propagation loss was estimated to be 0.13 dB/cm from the line slope in Fig. 2. This value is almost the same as that of the silica waveguide (0.07 dB/cm) having the same Δ as that of Bi-EDW. Since the loss level of the bismuthate channel waveguide was almost the same as that of silica waveguide,[11] we can say that the fabrication technology of multicomponent bismuthate glass waveguide has been established. According to this novel etching technology, we could achieve the smooth sidewall of core as shown in **Fig. 3**. In addition, the loss at the input and output connection points, which were spliced with high NA single mode fibers (Corning HI980) was estimated to be 0.5 dB/point by extrapolation of cut back method. This low connection loss value is due to matching of the mode field size between the Bi-EDW andthe HI980 fiber.

Next we report the gain characteristics of 6 cm long straight Bi-EDW with bidirectional pumping at 1480 nm. The pump power was 140 mW for each end and the input signal power was –10 dBm. The gain and noise figure spectra of a 6-cm long straight waveguide are shown in **Fig. 4**. A maximum gain of 6.8 dB was obtained at 1530 nm with a noise figure of 7.6 dB. Gain per unit length was calculated to be 1.1 dB/cm which is almost the same as that of Bi-EDF (1.1 dB/cm).

Although these values for the bismuthate fiber and waveguide are smaller than that of a phosphate glass waveguide, they are still larger than those of a silicate waveguide. These results indicate that this Bi-EDW has a potential for a compact amplifier from both points of view; high concentration of Er ions and small circuit with high Δ.

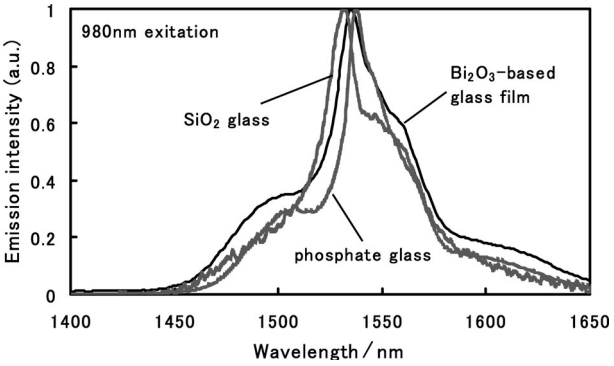

Fig. 1. Emission spectra of Er^{3+} ions glass doped in various glasses pumped at 980 nm.

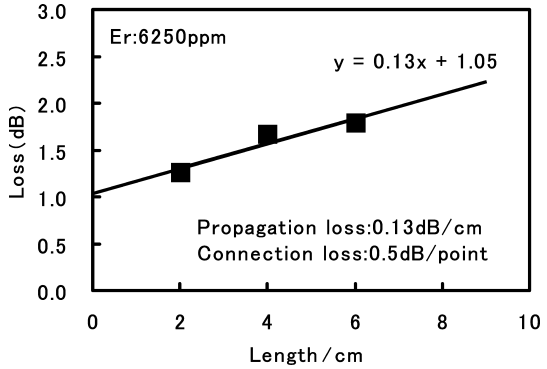

Fig. 2. Insertion loss of straight Bi-EDW at 1310 nm as a function of waveguide length.

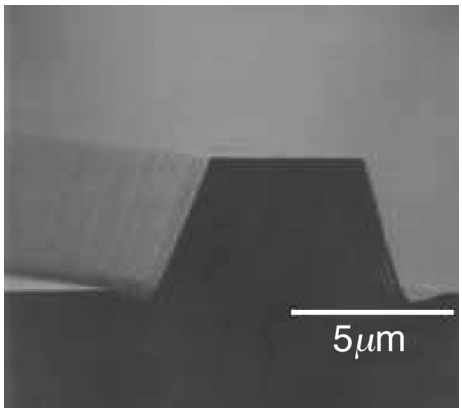

Fig. 3. Cross section of the core of Bi-EDW after dry-retching.

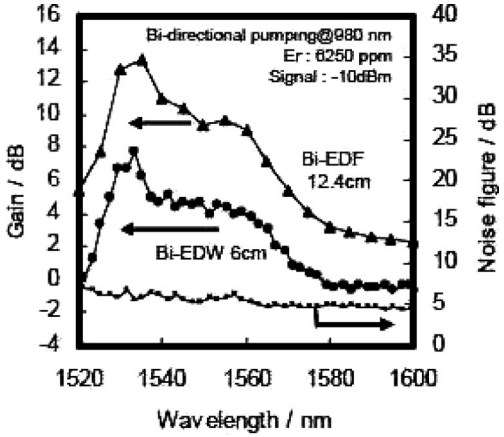

Fig. 4. Gain and noise figure of 6 cm long straight Bi-EDW pumped at 140 mW power as a function of wavelength.

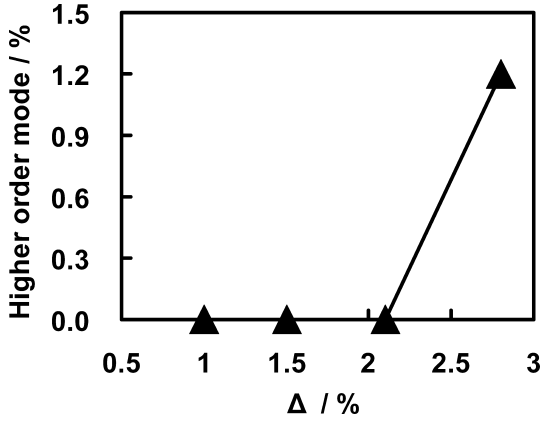

Fig. 5. Relationship between high order mode ratio and Δ for the waveguide which has 5 μm core width and 3.3 μm core height.

3.3 Simulation for single-mode condition

For design of waveguides, it is important to control Δ, which is the ratio of the refractive index difference between core and clad, to the core refractive index. In general, higher Δ is necessary for a compact waveguide because it can lead to low bending loss. On the other hand, too high Δ usually causes the deviation from the single-mode condition. Therefore, we simulated the relationship between single-mode condition and Δ. In general, the single-mode condition is derived from the Eq. (1)

$$\lambda = 2AN(2\Delta)^{1/2}. \quad (1)$$

where A is the core width and N is the core refractive index. In this calculation, the input beam was assumed to incident from all directions. Hence single-mode condition was estimated to be in a very narrow region. For example, when Δ is 2% and N is 1.9, the core width should be below 1.7 μm for 1310 nm. Since a narrower core width lead to lower coupling efficiency, we need to use wider core over 5 μm for better gain properties. If the incident beam is single-mode, we think that the single-mode condition of waveguide may be expanded. So we simulated the relationship between high order mode ratio and Δ when input beam was single-mode. **Figure 5** shows the relationship between high order mode ratio and Δ for the waveguide which has 5 μm core width and 3.3 μm core height. From this result, we found that the suitable Δ were in the range from 1.5% to 2.0%.

3.4 Simulation for bending loss

The curvature radius dependence of propagation loss of the waveguide was simulated by 2D-BPM. The structure of waveguide used to simulate was 90 deg-bending structure. **Figure 6** shows the relationship between curvature radius and bending loss for Δ is 1.5%. It is indicated that the bending loss is negligible when curvature radius is over 2 mm. So we set the minimum curvature radius to 2 mm.

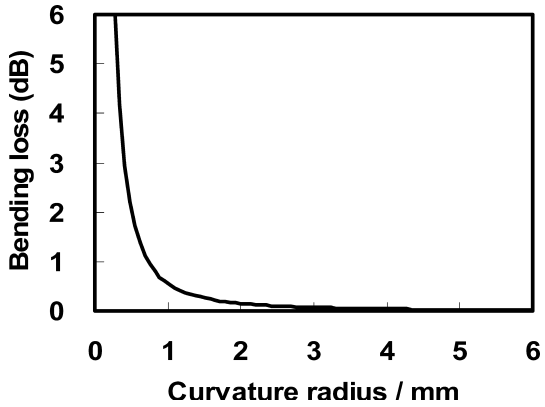

Fig. 6. Relationship between curvature radius and bending loss for 90 deg-bending structure which Δ is 1.5%.

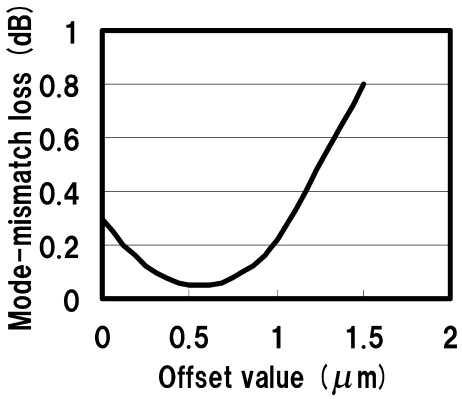

Fig. 7. Relationship between offset value and mode-mismatch loss at the inflection points consist of straight part and arc part whose curvature radius is 2 mm.

3.5 Simulation for offset structure

In a curved waveguide, the mode-center is not at the center of the core but shifted to outside of the center. There are some inflection points in the spiral waveguides. In particular, the square spiral waveguide has many inflection points at corner. At these many inflection points, loss arises from a mode-mismatch because the mode-center is not aligned. In order to reduce this mode-mismatch loss, offset structure were introduced. We simulated the relationship between offset value and mode-mismatch loss at the inflection point. The inflection point consist of a straight part and an arc part whose curvature radius is 2 mm. Simulation results are shown in **Fig. 7**. It can be seen that the minimum mode-mismatch loss is 0.08 dB for a 0.5 μm offset. To confirm the validity of the offset, we fabricated the waveguides include the offset structure and insertion loss was measured.

From the measurement result, the mode-mismatch loss was 0.15 dB. This value was larger than simulation result. The reason why this differential was that the offset structure could not be etched as same as photo mask pattern(dotted line) shown in **Fig. 8**. Thus, we contrived a novel offset structure to etch precisely and to be as effective as the conventional offset structure. The new offset structure is shown in **Fig. 9**. Figure 9 indicates that photo mask pattern(dotted line) and etched waveguide pattern are coincide. To confirm the validity of the new offset structure, we fabricated the waveguide include the new offset structure and insertion loss was measured. From the measurement result, the mode-mismatch loss was 0.08 dB. This value was consistent with the simulation result. From this result, we confirmed that the new offset structure could reduce mode-mismatch loss as calculated.

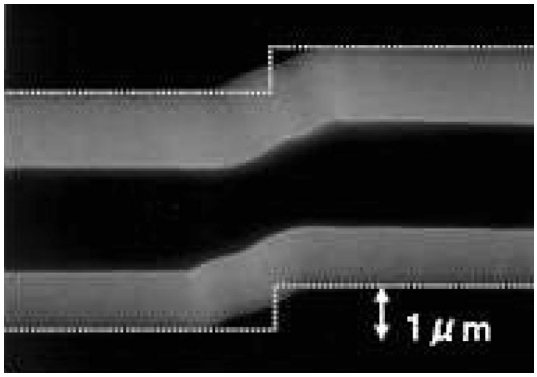

Fig. 8. SEM image of the offset part and conventional photo-mask pattern indicated by dotted line.

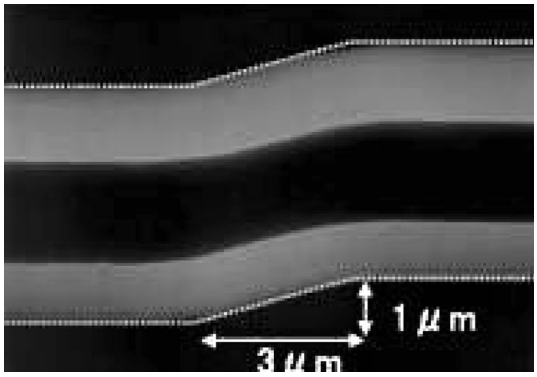

Fig. 9. SEM image of the offset part and new photo-mask pattern indicated by dotted line.

On the other hand, the circular spiral waveguide has only one inflection point at the center of the spiral pattern. We also simulated this case and concluded that the most suitable offset value was 1.0 μm. We also introduced the new offset structure in the circular spiral waveguide.

3.6 Characteristics of two spiral waveguides

Two optimally designed waveguides with different spiral layouts were shown in **Fig. 10**. We fabricated three waveguides of 16 cm, 25 cm, and 32 cm length respectively. **Figure 11** shows the relationship between spiral waveguide length and insertion loss. Square points indicate the square spiral waveguide and circular points indicate the circular spiral one. As expected, we found that the circular spiral waveguide had lower loss than the square one. And it shows that the propagation loss of square and circular spiral waveguide are 0.49 dB/cm and 0.15 dB/cm, respectively. Propagation loss of circular spiral waveguide is almost the same as that of straight waveguide. These results confirm that there is no bending loss in circular spiral waveguide. On the other hand, propagation loss of square spiral waveguide is high because of the many inflection points residual loss. Thus we found that the circular spiral layout was better than square one for insertion loss.

Next **Fig. 12** shows the relationship between spiral waveguide length and gain value at 1560 nm. Square points indicate the square spiral waveguide and circular points indicate the circular spiral one. We found that the circular spiral waveguide had higher gain value than the square spiral one. The gain shows maximum value at 25 cm long waveguide for each spiral layouts. From these results, we proposed that the 25 cm long circular spiral layout was most suitable for 1 cm^2 size Bi-EDWA. Single-mode propagation was confirmed by observation of FFP (Far Field Pattern) as shown in **Fig. 13**. MFD (Mode Filed Diameter) derived from FFP was nearly equal to simulation value.

Gain value and noise figure of 1 cm^2 size Bi-EDWA with 25 cm long shown in **Fig. 14**. Gain valueshigher than 15 dB with noise figures smaller than 8 dB are obtained in whole C-band region when input signal power is –10 dBm.

Picture of developed ultra-compact Bi-EDWA is shown in **Fig. 15**.

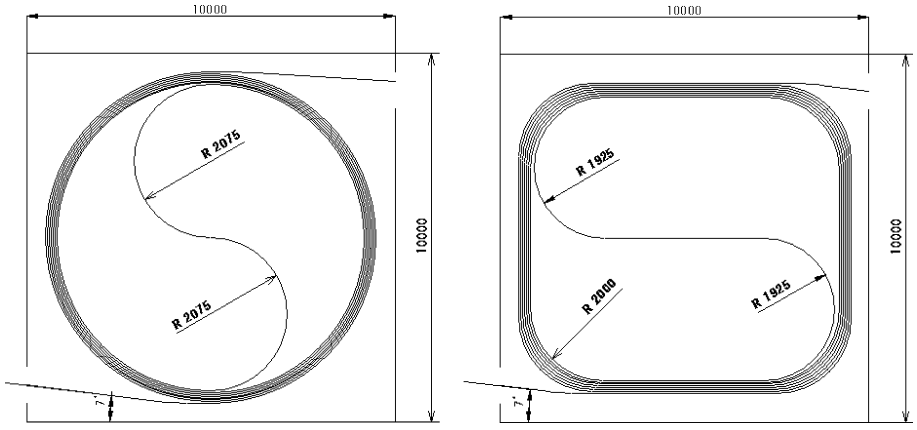

Fig. 10. Two optimal designed 1 cm-size waveguide with different spiral layouts.

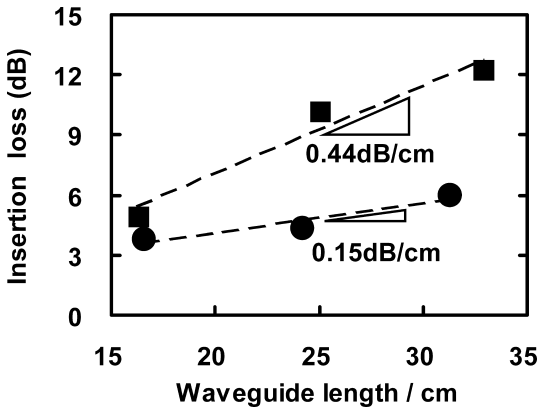

Fig. 11. Relationship between spiral waveguide length and insertion loss.

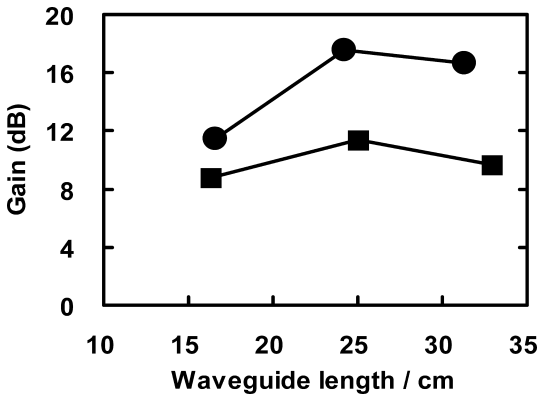

Fig. 12. Relationship between spiral waveguide length and gain value at 1560 nm.

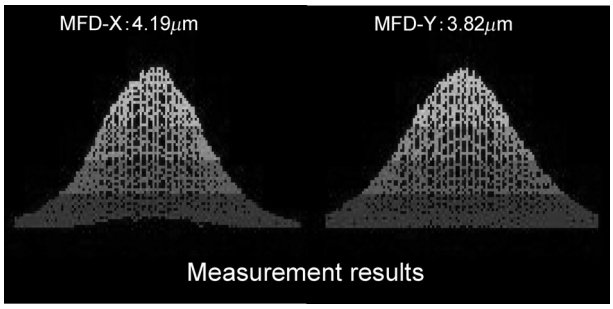

Fig. 13. FFP of 1 cm^2 size Bi-EDWA with 25 cm long.

4. Conclusions and summary

In this paper, we have reported the emission and gain characteristics of multicomponent bismuthate glass waveguide which has a potential for compact waveguide amplifier with flat and broad gain spectra. And we have established the etching technology of multicomponent bismuthate glass waveguide. According to that novel etching technology, we have been able to achieve the smooth sidewall and low loss waveguide. And net gain of 8 dB is obtained at 1530 nm by bidirectional pumping at 980 nm for 6 cm long waveguide.

Next we have reported the design and characteristics of ultra-compact Bi-EDWA. We have developed a 1 cm^2 size Bi-EDWA

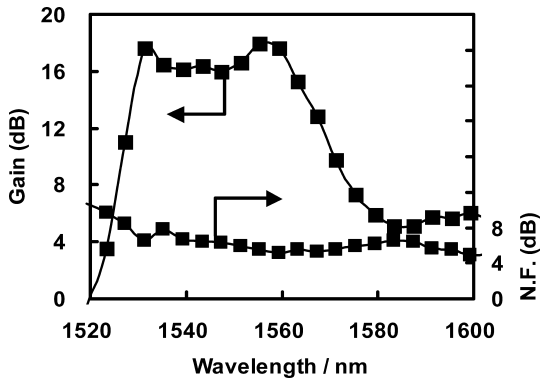

Fig. 14. Gain value and noise figure of 1 cm^2 size Bi-EDWA with 25 cm long.

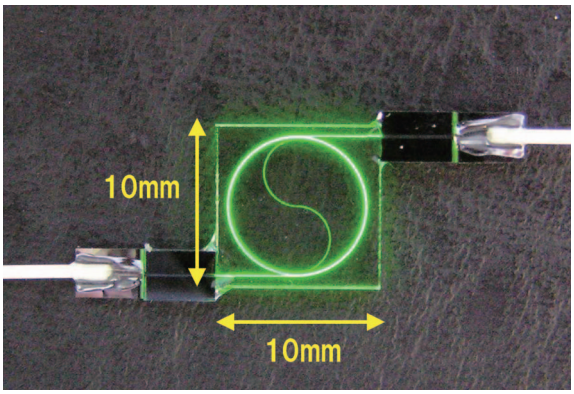

Fig. 15. Picture of developed ultra-compact Bi-EDWA.

which gain values and noise figure in whole C-band region are higher than 15 dB and smaller than 8 dB, respectively.

A part of this work has been performed under management of the OITDA supported by NEDO.

References

1) C. Qiao, Y. Chen and J. Staley, OFC2003, Atlanta (2003) p. TuJ5.
2) D. J. Blumenthal, J. E. Bowers, L. Rau, H. F. Chou, S. Rangarajan, W. Wei and H. N. Poulsen, *IEEE Comm. Mag.*, **41**, 23–29 (2003).
3) K. Motoshima, L. M. Leba, D. N. Chen, M. M. Downs, T. Li and E. Desurvire, *IEEE Photon. Tech. Lett*, 1423–1425 (1993).
4) N. Suzuki, T. Tokura, S. Kajiya, K. Shimizu and J. Nakagawa, ECOC2004 (2004) p. We.2.2.3.
5) Y. Kondo, M. Ono, J. Kageyama, M. Reyes, H. Hayashi and N. Sugimoto, OFC2005 (2005) Postdeadline paper, PDP2.
6) M. Ono, Y. Kondo, J. Kageyama, H. Hayashi and N. Sugimoto, OFC2006 Anaheim (2006) p. OTuD3.
7) K. Ennser, G. D. Valle, M. Ibsen, J. Shmulovich and S. Taccheo, *IEEE Photon. Tech. Lett.*, **17**, 1468–1470 (2005).
8) Y. Kondo, M. Ono, J. Kageyama, M. Reyes, H. Hayashi and N. Sugimoto, *Electronics Letters*, **41**, 317–318 (2005).
9) Y. Kondo, M. Ono, J. Kageyama and N. Sugimoto, OAA2005 (2005) MC2.
10) Y. Kondo, M. Ono, J. Kageyama and N. Sugimoto, ECOC2006 (2006) p. We2.6.4.
11) S. Senichi, M. Yanagisawa, Y. Hibino and K. Oda, *J. Lightwave Tech.*, **12**[5], 790–796 (1994).